THREE-DIMENSIONAL THERMAL FILTRATION STUDY OF WATER CONING CONTROL

Bakhbergen E. Bekbauov[1], Aidarkhan Kaltayev[1]
[1]*Al-Farabi Kazakh National University, Almaty, Kazakhstan*
e-mail: Bakhbergen.Bekbauov@kaznu.kz

Abstract

A numerical thermal study of heavy oil recovery process developed in this work to investigate the time dependent development and dynamic shape of the water-oil interface around the well producing from a bottom-water-drive homogenous reservoir. Observed were the effects of well completions (single or dual – with the bottom water drainage) and impermeable barrier injected around the well bore on water coning.

Introduction

To describe thermal treatment of pools, the temperature model of two-phase filtration [1] based on the Muskat-Leverett isothermic model (the MLT model) was used. The model takes heat effects into account via the known dependences on the viscosity, and capillary properties of the two-phase liquid (water-oil) components. System of equations describing the process also includes the contribution of gravity forces. Author was the first to consider 3D cylindrical thermal two-phase filtration model taking into account all terms of the existing mathematical model including barrier-drainage system investigation. Dimensionless parameters were derived from the governing equations in view of physical characteristics of flow. The author also proposes a new formula for approximation of Leverett J-function which is convenient to use in numerical experiments from his point of view. The main advantages of this formula are related to the facts that it able to quite precisely approximate any monotonically decreasing smooth function by selection constants, and also unlike some formulas its derivative is not equal to infinity at zero. Observed was the effect of well completions on water coning in four different reservoir settings. The first was a case of conventional completion and was studied as a base case. In the second case was set dual completion with water drainage. The third scenario was an impermeable barrier injected around the well bore. In the fourth case was considered complex effect of dual completion with water drainage and impermeable barrier. Siddiqi and Wojtanowicz used a scaled physical model and numerical simulator to determine the effect of artifical barrier and downhole water sink technology on water coning performance [2]. This work was taken as a source of results for comparison.

Mathematical Model

The MLT model [3] of the two-phase immiscible fluids' (water and oil) flow through a porous medium is much more complex than Darcy's model. Continuity equations and generalized Darcy's model for each fluid component can be written in the form:

$$\frac{\partial}{\partial t}\left(m_0 \rho_i s_i\right) + div\left(\rho_i \vec{v}_i\right) = 0 , \; \vec{v}_i = -K_0 \frac{\bar{k}_i}{\mu_i}\left(\nabla p_i + \rho_i \vec{g}\right), \qquad i = 1,2$$

Hence (indexes $i = 1, 2, 3$ correspond respectively water, oil and porous medium below):

$$m\frac{\partial s}{\partial t} = div\left[a_1 \nabla s + \vec{f}_1 + a_2 \nabla \theta\right], \; div\left(K \nabla p + \vec{f}_2 + a_3 \nabla \theta\right) = 0$$

$$-\vec{v} = K \nabla p + \vec{f}_2 + a_3 \nabla \theta , \qquad \frac{\partial \theta}{\partial t} = div\left[\lambda(x, s, \theta)\nabla \theta - \vec{v}\theta\right],$$

$m = m_0(1 - s_1^0 - s_2^0)$, m_0 - porosity

s_i^0, $i = 1,2$, residual water and oil saturations respectively

$s = \dfrac{s_1 - s_1^0}{1 - s_1^0 - s_2^0} \in [0,1]$, s_i - saturation, $i = 1,2$; $s_1 + s_2 = 1$;

$0 < s_i^0 \le s_i \le 1 - s_j^0 < 1, \quad i \ne j$

t - time

$a_1 = -K_0 \dfrac{k_1 k_2}{k} \dfrac{\partial p_c}{\partial s}$

K_0 - symmetrical flow tensor of an anisotropic porous medium. In the case of anisotropic porous medium K_0 can be expressed via k_h - horizontal permeability and k_v - vertical permeability components of symmetrical flow tensor.

$k_i = \dfrac{\bar{k}_i}{\mu_i}$; $0 \le \bar{k}_i \le 1$ - relative permeabilities

$\bar{k}_i(s_i^0) = 0, \quad i = 1,2$; $\bar{k}_i(s) > 0, \quad s \in (0,1)$; $\bar{k}_1(0) = \bar{k}_2(1) = 0$.

μ_i - dynamic viscosity coefficient ($\mu_1 = const$);

$$\mu_2 = \mu_{2\max} + (\mu_{2\min} - \mu_{2\max}) \frac{\theta - \theta_{\min}}{\theta_{\max} - \theta_{\min}}$$

θ - temperature; $k = k_1 + k_2$;

$$p_2 - p_1 = p_c(x, s, \theta) \ge 0;\; p_c(x, s, \theta) = \bar{p}_c(x, \theta) J(s);\; \bar{p}_c = \sigma \cos\vartheta \left(\frac{m_0}{|K_0|} \right)^{1/2} = \gamma(\theta) \left(\frac{m_0}{|K_0|} \right)^{1/2}$$

where σ - interfacial tension coefficient, ϑ - wetting angle, $|K_0|$ - determinant of matrix $\{k_{i,j}\}$, $\gamma = \gamma_{\max} + (\gamma_{\min} - \gamma_{\max}) \dfrac{\theta - \theta_{\min}}{\theta_{\max} - \theta_{\min}}$; $J(s)$ - Leverett function.

$$\vec{f}_1 = K_1 \left(\nabla p + \int_s^1 \nabla \frac{\partial p_c}{\partial s} \frac{k_2}{k} ds \right),\; K_i = K_0(x) k_i(s) = K_0(x) \frac{\bar{k}_i(s)}{\mu_i}.$$

$$p = p_1 - \int_s^1 \frac{\partial p_c}{\partial s} \frac{k_2}{k} ds + \rho_1 g h$$

ρ_i - density, (both fluids are assumed to be incompressible, i.e. $\rho_i = const$)

g - acceleration of gravity

h - height

$$a_2 = K_1 \int_s^1 \frac{\partial}{\partial \theta} \left(\frac{\partial p_c}{\partial s} \frac{k_2}{k} \right) ds$$

$$\int_s^1 \frac{\partial}{\partial \theta} \left(\frac{\partial p_c}{\partial s} \frac{k_2}{k} \right) ds = \sqrt{\frac{m_0}{K_0}} \int_s^1 J'(s) \left\{ \frac{\gamma_{\min} - \gamma_{\max}}{\theta_{\max} - \theta_{\min}} \frac{k_2}{k} - \gamma \frac{k_1 k_2}{\mu_2 k^2} \left(\frac{\mu_{2\min} - \mu_{2\max}}{\theta_{\max} - \theta_{\min}} \right) \right\} ds$$

$K = K_0 k = K_0 (k_1 + k_2)$

$$\vec{f}_2 = K \int_s^1 \nabla \frac{\partial p_c}{\partial s} \frac{k_2}{k} ds + K_2 (\nabla p_c + (\rho_2 - \rho_1) \vec{g})$$

$$a_3 = K\int_s^1 \frac{\partial}{\partial\theta}\left(\frac{\partial p_c}{\partial s}\frac{k_2}{k}\right)ds + K_2\nabla\theta$$

$$\vec{v} = \vec{v}_1 + \vec{v}_2$$

$$-\vec{v} = K\nabla p + K\int_s^1 \nabla\frac{\partial p_c}{\partial s}\frac{k_2}{k}\,ds + K_2\nabla p_c + K_2(\rho_2-\rho_1)\vec{g} + K\int_s^1 \frac{\partial}{\partial\theta}\left(\frac{\partial p_c}{\partial s}\frac{k_2}{k}\right)ds\nabla\theta + K_2\frac{\partial p_c}{\partial\theta}\nabla\theta$$

$\vec{v}_i$ - velocity, $-v_1 = -K_0\frac{k_1k_2}{k}\frac{\partial p_c}{\partial s}\nabla s + K_1\nabla p + K_1\int_s^1 \nabla\frac{\partial p_c}{\partial s}\frac{k_2}{k}ds + K_1\int_s^1 \frac{\partial}{\partial\theta}\left(\frac{\partial p_c}{\partial s}\frac{k_2}{k}\right)ds\nabla\theta$

$\lambda(s,\theta) = \sum_{i=1}^{3}\frac{\alpha_i\lambda_i}{\rho_i c_{pi}}$, $\alpha_1 = m_0 s_1$, $\alpha_2 = m_0(1-s_1)$, $\alpha_3 = 1-m_0$.

λ_i - thermal conductivity (i=1,2,3, respectively water, oil and core)

c_{pi} - heat capacity coefficient of i-phase at constant pressure.

For the proposed Leverett function formula $J(s) = \frac{1}{b+(a-b)\cdot s^{\alpha}} - c\cdot s^{\beta}$ were taken following constants: $a=5$; $b=0.2$; $c=0.2$; $\alpha=1$; $\beta=500$.

Model Description

Table 1 – Description of the Cases analyzed in this study

Cases considered	Description
Case 1	W/o barrier and w/o drainage
Case 2	W/o barrier and with drainage
Case 3	With barrier and w/o drainage
Case 4	With barrier and with drainage

Table 2 - Reservoir geometry, rock and fluid properties considered for the all 4 cases

Property	**Denotation (Unit)**	**Value**
Reservoir Radius	R (m)	40
Total Thickness of the Reservoir	H (m)	20
Initial Water Zone Thickness	Hw (m)	10
Initial Oil Zone Thickness	Ho (m)	10
Well Penetration Thickness	Hp (m)	4.5
Water Viscosity	μ_1 (cp)	0.5
Oil Viscosity at $\theta_{\min}$	$\mu_{2\max}$ (cp)	5
Oil Viscosity at $\theta_{\max}$	$\mu_{2\min}$ (cp)	1
Maximum Surface Tension at $\theta_{\min}$	σ kg/s^2	0.03
Minimum Surface Tension at $\theta_{\max}$	σ kg/s^2	0.015
Horizontal Permeability	k_h (darcies)	2
Vertical Permeability	k_v (darcies)	0.6
Relative Permeabilities	(1 – water, 2 - oil)	$\overline{k_1} = s^2$, $\overline{k_2} = (1-s)^2$
Porosity	m_0 (fraction)	0.25

Irreducible (Residual) Water Saturation	s_1^0 (fraction)	0.2
Residual Oil Saturation	s_2^0 (fraction)	0.2
Total (Liquid) Production Rate in the Oil Zone	q_1 (b/d)	1000
Water Production Rate in the Water (Drainage) Zone	q_2 (b/d)	3000
Water Density	$\rho_1\left(kg/m^3\right)$	1000
Oil Density	$\rho_2\left(kg/m^3\right)$	730
Rock Density	$\rho_3\left(kg/m^3\right)$	4216
Thermal Conductivity of Water	$\lambda_1\left(W/(m\cdot K)\right)$	0.644
Thermal Conductivity of Oil	$\lambda_2\left(W/(m\cdot K)\right)$	0.08
Thermal Conductivity of Core	$\lambda_3\left(W/(m\cdot K)\right)$	2.4
Specific Heat Capacity Coefficient of Water at Constant Pressure	$c_{p1}\left(J/(kg\cdot K)\right)$	4071
Specific Heat Capacity Coefficient of Oil	$c_{p2}\left(J/(kg\cdot K)\right)$	2100
Specific Heat Capacity Coefficient of Core	$c_{p3}\left(J/(kg\cdot K)\right)$	920
Initial Reservoir Pressure (Modified Pressure)	p (Pa)	$25\cdot 10^6$
Initial Water Zone Temperature	θ (K)	350
Initial Oil Zone Temperature	θ (K)	330

Computer Simulation Results

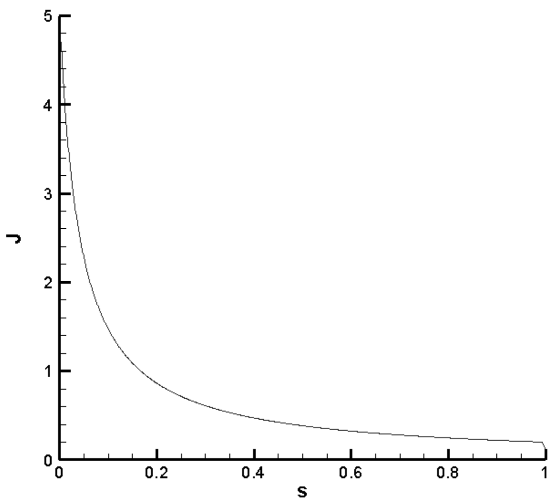

Figure 1 - Leverett Function Used in the Simulation Model

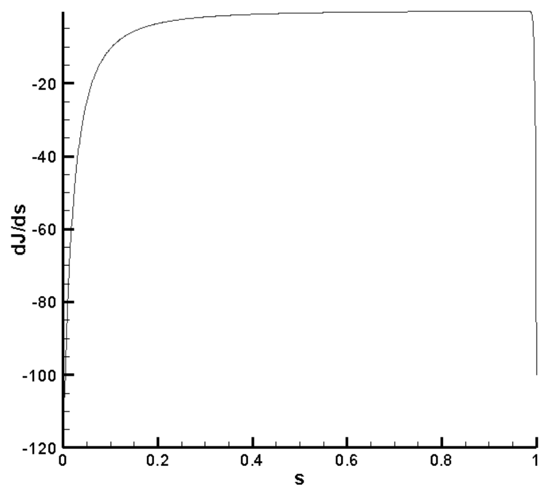

Figure 2 – Derivative of Leverett Function

To demonstrate the radial effect, barrier with various radius (r=10 m at $\varphi=\left[-120^0,120^0\right]$ and r=5 m at $\varphi=\left(120^0,240^0\right)$) was used which is illustrated in Figure 3 below:

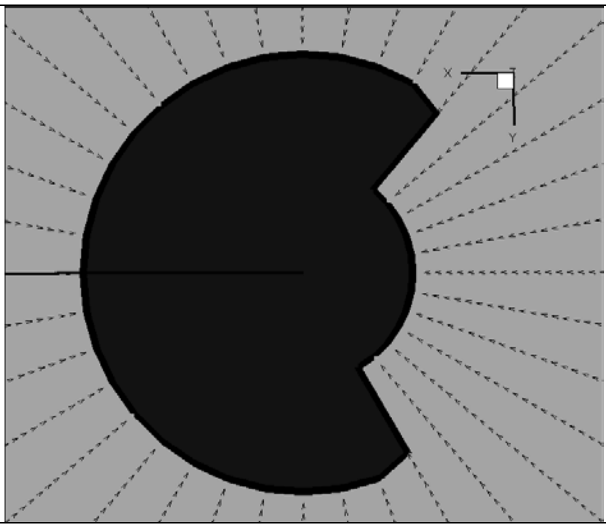

Figure 3 - Barrier design. View from upstairs

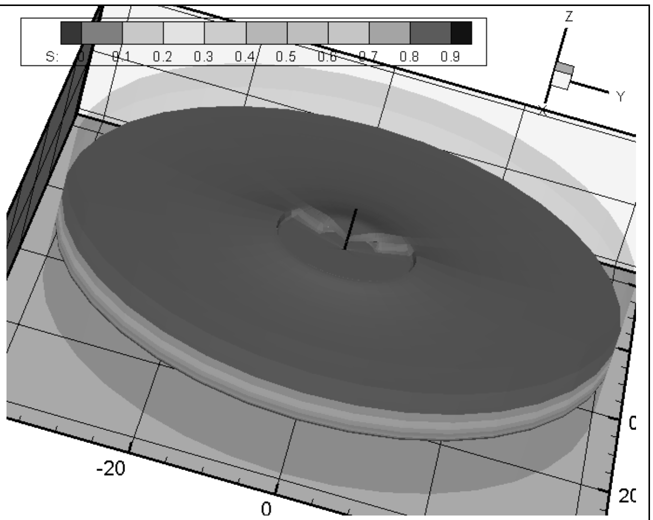

Figure 4 – Water saturation isosurfaces at t = 91hours (Case 3)

Figures 5.1 – 5.4 show the distribution of different water saturation isosurfaces at the breakthrough times for each cases analyzed in this study. All figures show $0^0 - 180^0$ cross-section of the reservoir.

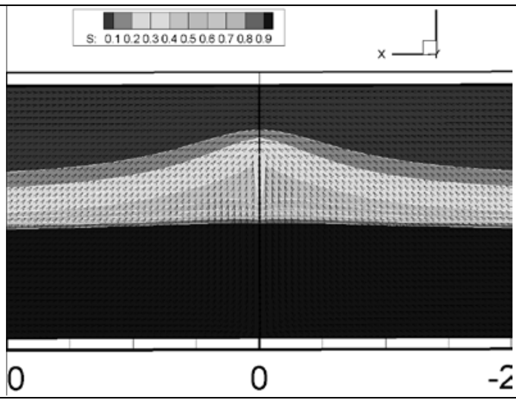

Figure 5.1 – Water saturation distribution and velocity field at t = 91 hours

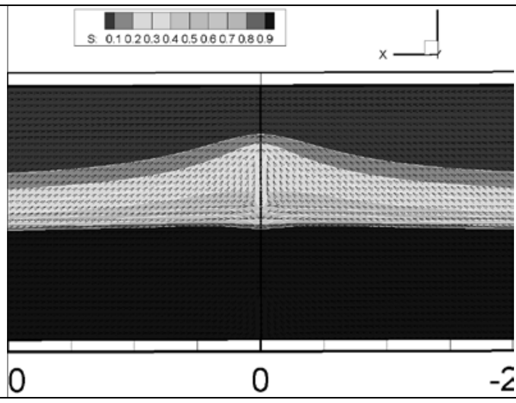

Figure 5.2 – Water saturation distribution and velocity field at t = 91 hours

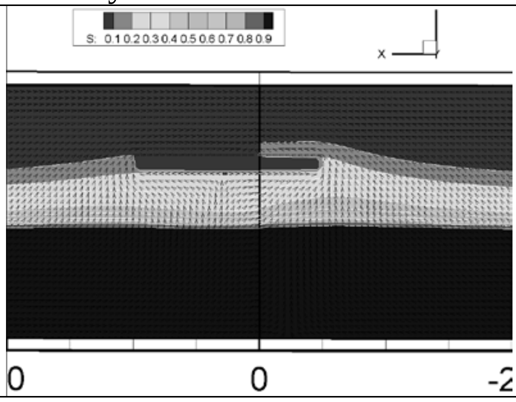

Figure 5.3 – Water saturation distribution and velocity field at t = 91 hours (breakthrough)

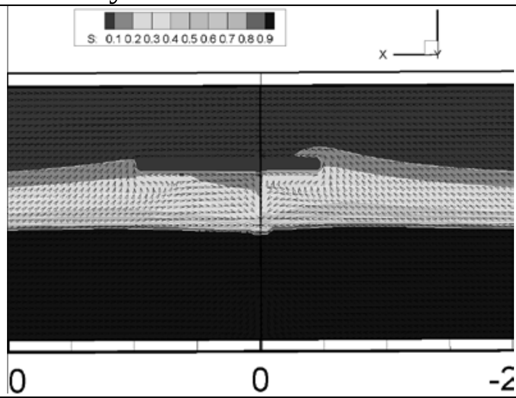

Figure 5.4 – Water saturation distribution and velocity field at t = 91 hours

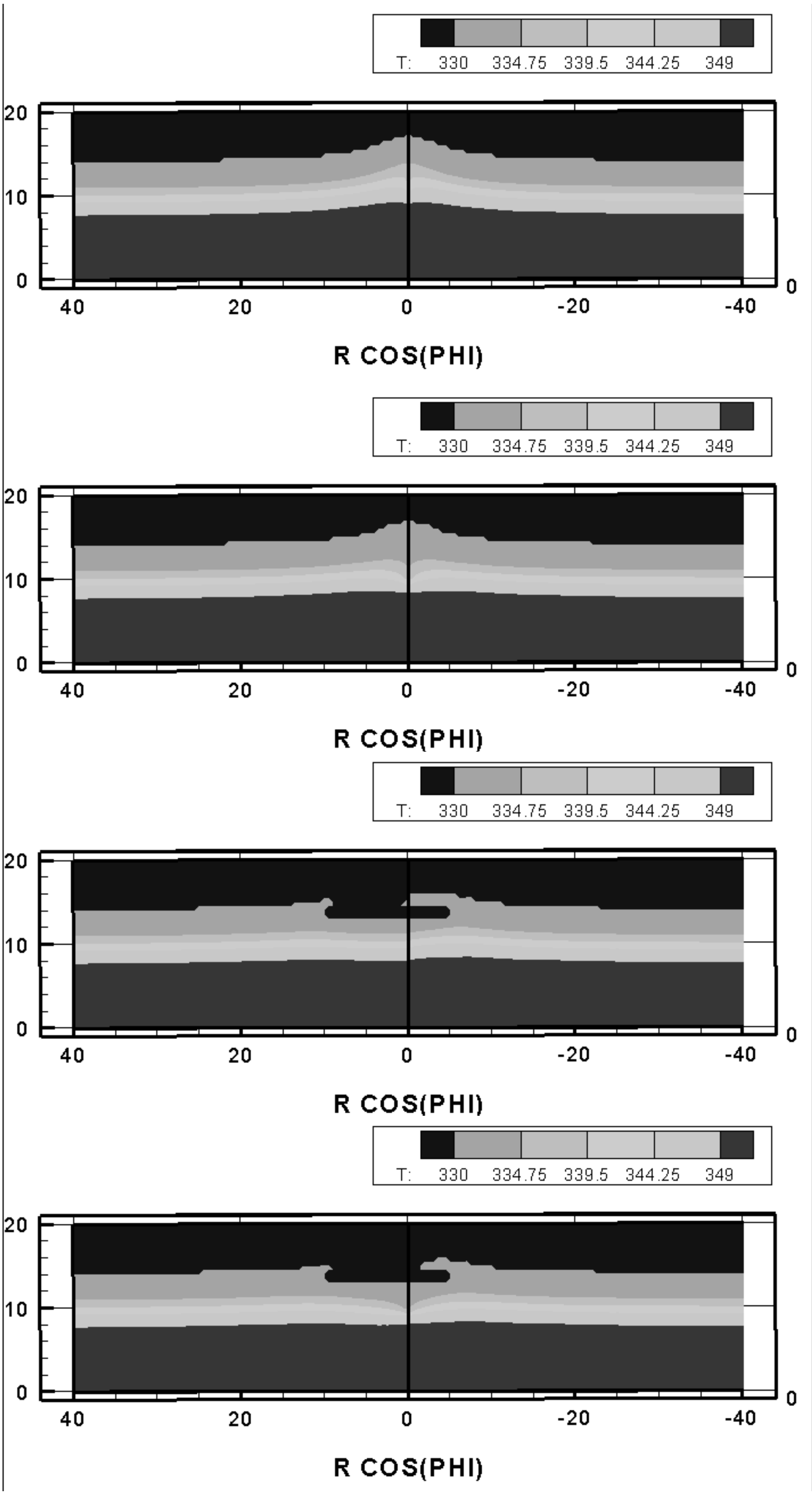

Figure 6 – Temperature field distribution at t = 16 days (384 hours) for Cases 1,2,3,4 respectively

Figures 7, 8 show results of 3D reservoir simulation:

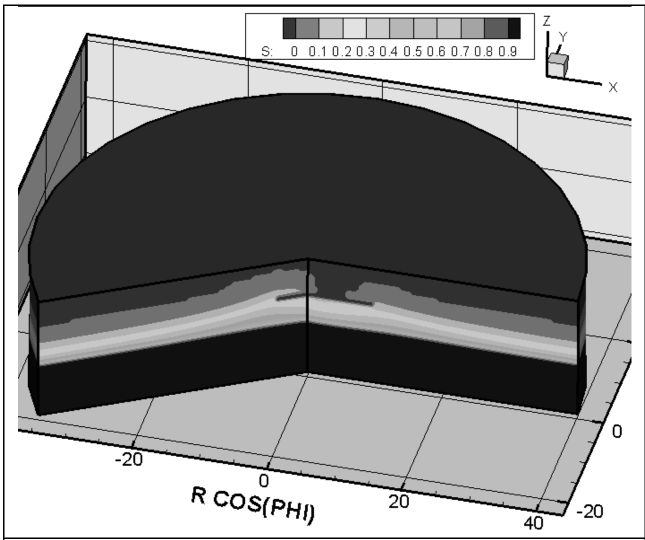

Figure 7 – Water saturation distribution at t = 85 h

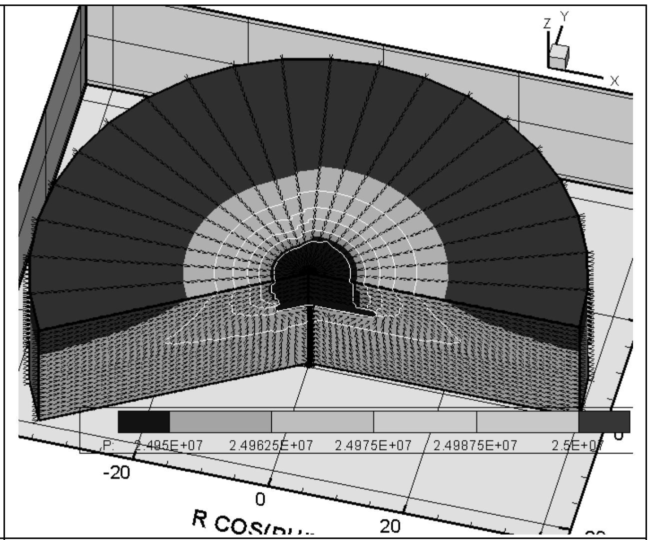

Figure 8 – Pressure and velocity distribution at t = 90 h

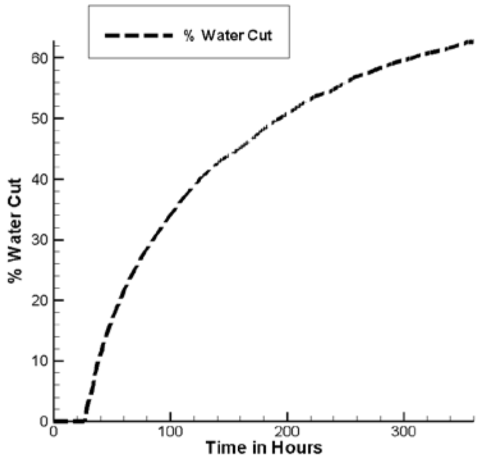

Figure 9 – Case 1

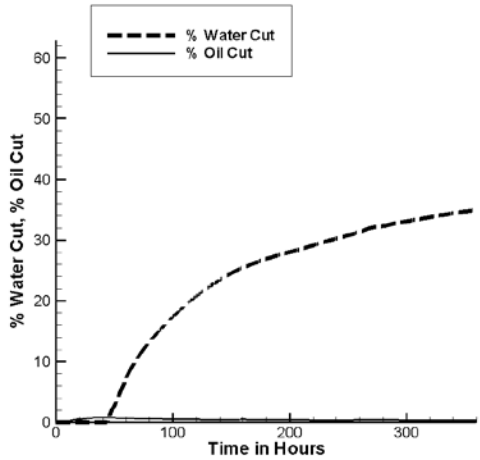

Figure 10 – Case 2

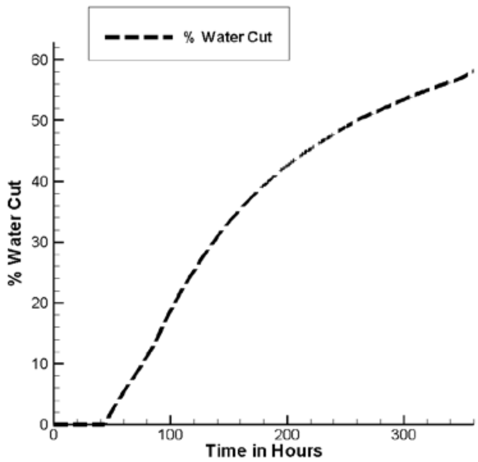

Figure 11 – Case 3

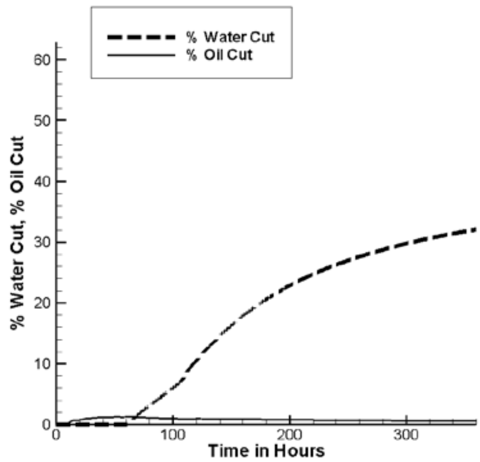

Figure 12 – Case 4

Conclusion

The comparison of results from this work and the work carried out by Siddiqi et. al. [2] suggests that a novel model can be used to study the effect of an impermeable barrier and downhole water sink technology on the coning phenomenon. The results could help in selecting methods for specific reservoir conditions (see figures 9-12).

The study revealed that placing a man-made impermeable barrier around the well bore would delay the water breakthrough and, thus, can be useful in increasing the period of water free oil. Study also showed that breakthrough time was directly proportional to the radius of gel barrier. The results from this model showed that although placement of such a layer delays the breakthrough of water, it does not stop water-coning process. In case of high oil production rate, the water simply goes around the barrier's top and breaks to the well's completion. After the water breakthrough, the reservoir system behaves in the same way as if there was no barrier, i.e. the final water-cut value in the barrier case is the same as in the no barrier case.

The study revealed that in the homogenous reservoir, using dual completion, it was possible to decrease water-cut in the oil production by draining water from the bottom completion and producing oil from the top completion. This study also confirms the fact that has been established by earlier studies: dual completion can stop water coning but for doing that the water production rate from the drainage has to be much higher than the oil production rate.

It was observed that DWS technique has not high efficiency in controlling water coning in the presence of an impermeable barrier around the well bore as the barrier stops the pressure communication between the sink and the production completion. Hence the results obtained from the novel 3D model agree with the physical model (the experimental data) as well as with results of numerical simulator.

REFERENCES

1. Bocharov O.B., Telegin I.G. "Numerical modeling of thermo-capillary countercurrent impregnation". Thermo physics and aeromechanics, 2005, volume 12, № 3.
2. Siddiqi, S. S. and Wojtanowicz, A. K.: "A Study of Water Coning Control in Oil Wells by Injected or Natural Flow Barriers Using Scaled Physical Model and Numerical Simulator", SPE 77415, presented at the SPE Annual Technical Conference and Exhibition held in San Antonio, Texas, 29 September–2 October 2002.
3. Zhumagulov B.T., Monakhov V.N. "The Fluid Dynamics of Oil Production": Translated & ed. by AgipK CO. – Milan: Interservice, 2003 – 307 p., etc.